PHYSICAL REVIEW C **87**, 014326 (2013)

Three-quasiparticle isomers and possible deformation in the transitional nuclide, ^{195}Au

G. D. Dracoulis,[1] G. J. Lane,[1] H. Watanabe,[1,2,*] R. O. Hughes,[1,†] N. Palalani,[1] F. G. Kondev,[3] M. P. Carpenter,[4] R. V. F. Janssens,[4] T. Lauritsen,[4] C. J. Lister,[4] D. Seweryniak,[4] S. Zhu,[4] P. Chowdhury,[5] W. Y. Liang,[6] Y. Shi,[6] and F. R. Xu[6]

[1]*Department of Nuclear Physics, R.S.P.E., Australian National University, Canberra, A.C.T. 0200, Australia*
[2]*RIKEN Nishina Center, 2-1 Hirosawa, Wako, Saitama 351-0198, Japan*
[3]*Nuclear Engineering Division, Argonne National Laboratory, Argonne Illinois, USA*
[4]*Physics Division, Argonne National Laboratory, Argonne, Illinois, USA*
[5]*Department of Physics, University of Massachusetts Lowell, Lowell, Massachusetts 01854, USA*
[6]*School of Physics, Peking University, Beijing 100871, China*

(Received 21 December 2012; published 22 January 2013)

Deep-inelastic reactions and γ-ray spectroscopy have been used to study excited states in ^{195}Au. A three-quasiparticle isomer with a mean-life of 18.6(3) μs has been assigned at $2461 + \Delta$ keV, with decays into newly identified structures. Possible configurations for the isomer are discussed including a $J^\pi = 31/2^-$ intrinsic state produced by coupling the $11/2^-[505]$ proton hole to the 10^+ state obtained from the $9/2^+[624]$,$11/2^+[615]$ two-neutron holes, expected from configuration-constrained potential-energy-surface calculations. Residual interactions are evaluated within a semi-empirical shell model basis. New lifetime information is also obtained for the $21/2^+$ and $25/2^+$ states at 1813 and 1980 keV. The relationship between these and other newly identified states and the negative-parity states in the even-even neighbors is discussed.

DOI: 10.1103/PhysRevC.87.014326 PACS number(s): 21.10.Re, 21.10.Tg, 23.20.Lv, 27.80.+w

I. INTRODUCTION

The gold isotopes ($Z = 79$) lie just beyond the region of well deformed nuclei and fall across a well known prolate-to-oblate shape transition near $N = 116$ and $Z = 78$ [1]. This is also a region where triaxiality in the even-even isotopes may be manifested [2,3] and where, in general, the preferred deformation is sensitive to both the occupation of specific orbitals and to the dynamics introduced by rotation. In this context, it should be noted that, while the odd-A isotopes near ^{195}Au were predicted originally by Moller *et al* [4] to be weakly oblate (with $\epsilon_2 \sim -0.13$), their extended calculations that include asymmetry predict triaxiality with $\gamma = 30^o$ [5]. However, neither of these calculations is specific about which orbitals are occupied.

The structure and shape of multiparticle states in particular will be sensitive to the combination of active protons and neutrons. The proton Fermi surface lies close to the (mixed) $d_{3/2}$ orbital but it is also at the top of the unique-parity $h_{11/2}$ shell. Therefore, prolate high-spin (high-K) structures are likely to involve the high-Ω, $11/2^-[505]$ orbital. In contrast, the proximity to the low-Ω, $1/2^-[550]$ orbital at oblate deformation favors rotation aligned structures, a maximum of $10\hbar$ of angular momentum being available from the full alignment of a pair of $h_{11/2}$ protons. Proton alignment can also occur at prolate deformation through the population of the $h_{9/2}$ low-Ω orbitals that intrude from above the $Z = 82$ shell.

The neutron situation is similar: the Fermi level relative to the $i_{13/2}$ neutron shell is in a position analogous to that of the protons in the $h_{11/2}$ shell, resulting in the possibility of high-K structures, with a maximum of $K = 12$ obtained by summing the $11/2^+[615]$ and $13/2^+[606]$ orbital projections. Competing oblate rotation-aligned structures have $12\hbar$ available from the alignment of a pair of $i_{13/2}$ neutrons. The mixed $f_{7/2}/h_{9/2}$ configuration, deeper below the closed shell, also gives rise to the high-Ω, $9/2^-[505]$ and $7/2^-[503]$ orbitals located near the neutron Fermi surface at prolate deformation.

Except for the $h_{9/2}$ protons, most of the key orbitals are hole-like and have different deformation-driving properties. The study of isomeric high-spin states provides, in principle, a way of isolating some of these nuclear structure effects, possibly with less ambiguity than might be the case through the study of band structures alone. Our recent study [6] of long-lived isomers in the odd iridium isotopes, including ^{193}Ir, the isotone of ^{195}Au, resulted in their association with the relatively stable triaxially deformed structures predicted by configuration-constrained potential-energy-surface (PES) calculations [6].

For a purely spherical shape, the high-spin two-neutron one-proton structures that can be formed correspond to the $\nu i_{13/2}^{-1}(p_{3/2}/f_{5/2})^{-1} \otimes \pi h_{11/2}^{-1}$ and $i_{13/2}^{-1}h_{9/2}^{-1} \otimes \pi h_{11/2}^{-1}$ multiplets, with near-maximum and maximum spins of $27/2^+$ and $29/2^+$ in the first case, and $31/2^+$ and $33/2^+$ in the second. Which of these would be energetically favored depends in part on their hole/particle-like nature and the associated residual interactions.

For the case of the $N = 116$ isotope, ^{195}Au, previous experimental information was limited until recently to β-decay work and to the (α,$2n$) fusion-evaporation studies of Tjøm *et al*. [7]. The latter studies were able to reach states with medium spins in the negative-parity bands and included the identification of a relatively short-lived ($T_{1/2} = 8$ ns), $21/2^+$ isomeric state at 1813 keV.

The nuclear structure interpretation of Ref. [7] was proposed largely in the context of the rotation-aligned coupling scheme and the "decoupled" bands expected to arise, as

*Present address: School of Physics and Nuclear Energy Engineering, Beihang University, Beihang 100191, China.
†Present address: Department of Physics, University of Richmond, 28 Westhampton Way, Richmond, Virginia 23173, USA.

indicated above, when the proton Fermi level is close to the $\Omega = 1/2$ orbital of the $h_{11/2}$ proton configuration. This situation occurs at *oblate* deformation, under conditions that maximize the Coriolis effects [8]. The level sequences, $11/2^-$, $15/2^-$, $19/2^-$, ... that arise have spacings that mimic those of the ground-state bands in the even-even Hg neighbors (but are not to be confused with weak coupling). As mentioned earlier [7] and quantified in later studies, the detailed band structure suggests triaxiality rather than oblate deformation, but the general interpretation in terms of rotation alignment holds. Recent total Routhian surface (TRS) calculations for the negative-parity states in the range of gold isotopes from ^{189}Au to ^{197}Au indeed indicate triaxality (depicted in Ref. [9] at a frequency of 0.127 MeV) but with potential minima that become more localized at oblate deformation with increasing neutron number.

The authors of Ref. [9] conjectured that an isomer in ^{195}Au might be expected, similar to the $J^\pi = 31/2^+, T_{1/2} = 150(5)$ ns state in ^{193}Au [10], largely on the basis of systematics. The configuration of such an isomer, formed by coupling the $11/2^-[505]$ proton to the 10^- neutron-core structure, is the same as the one we proposed for the long-lived isomers identified in ^{191}Ir and the isotone of ^{195}Au, ^{193}Ir [6]. However the 10^- structure is predicted to rise rapidly in excitation energy near $N = 116$ and the energy depends sensitively on deformation. In fact, in the iridium cases, it was shown that both $31/2^-$ and $31/2^+$ three-quasiparticle structures were to be expected in the same energy region. These issues will be discussed in more depth later in this report, in the context of ^{195}Au.

On the experimental side, in a study aimed mainly at ^{197}Au, Wheldon *et al.* [11] identified a 482-keV delayed γ ray in ^{195}Au that purportedly fed the $21/2^+$ isomeric state, but they did not establish a more detailed scheme. Wang *et al.* [9] recently also reported results for ^{195}Au from the ^{192}Os(^{7}Li, $4n$) reaction including placement of the 482-keV transition as a branch from a 2461-keV state, but they did not identify any new isomers.

II. EXPERIMENT AND DATA ANALYSIS

The studies reported here draw on the ability of so-called "deep inelastic" heavy-ion reactions to populate high-spin states in a broad range of nuclei through either inelastic excitation or transfer of a few particles between a particular projectile and target nucleus [12]. The experimental configuration where reaction products are stopped in the target is most effective for the population and identification of states that are either long-lived or are fed by isomers. In this arrangement, the direct identification of very short-lived states (ps range) is limited by Doppler broadening.

Details of our measurements, using similar experimental configurations and analysis techniques, have been given in a number of publications (e.g., Refs. [6,13,14]) where more information can be found. The measurements used ~6.0 MeV/u ^{136}Xe beams provided by the ATLAS facility at Argonne National Laboratory. Nanosecond pulses, separated by 825 ns, were incident on a variety of targets, all mounted with a gold foil directly behind them, and, in the case of the ^{192}Os target, with a gold mask on the front in order to center the small-area target. The majority of the present results were obtained with the last configuration in which the extremities of the beam spot can strike the gold mask with the maximum beam energy whereas, in the other cases, the beam loses energy in the primary target before reaching the gold backing.

Gamma rays were detected using Gammasphere [15], with 100 detectors in operation. Triple coincidence events were required and the main data analysis was carried out with γ-γ-γ cubes, using various time-difference conditions, and also with time constraints relative to the pulsed beam, allowing selection of different out-of-beam regimes, as detailed in Refs. [6,13,14].

Another set of measurements was carried out using a macroscopically chopped beam with adjustable beam-on/beam-off conditions. In these, out-of-beam dual coincidence events were recorded in reference to a precision clock and γ-γ matrices as a function of time were constructed for contiguous time regions, allowing long lifetimes to be isolated by gating on cascades within a specific nucleus. Scans were made under different experimental conditions, progressing in steps of ten, from initial values in the submillisecond range up to the region of a few seconds, the maximum that could be accommodated by the electronics. The main results reported here were obtained with the 100/400 μs configuration.

To aid with spectroscopic assignments, total conversion coefficients were deduced from (delayed) intensity balances. In conjunction with the usual considerations of γ-ray branching and transition strengths, γ-γ angular correlations were also used to constrain spins and parities. (See Ref. [13] for details of the angular correlation technique.)

III. RESULTS AND LEVEL SCHEME

Figure 1 provides a spectrum with a double coincidence gate on a pair of the known low-lying yrast transitions, and an additional time gate to select out-of-beam γ rays. The level scheme deduced for ^{195}Au is given in Fig. 2. Most of

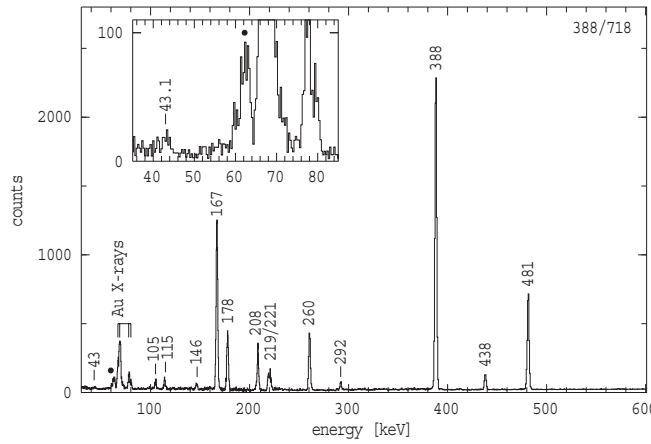

FIG. 1. Out-of-beam γ-ray spectrum with a double γ-ray coincidence gate on the 388- and 718-keV lines in ^{195}Au. A strong 388-keV line is observed because of the unresolved doublet of cascade γ rays at this energy. The inset shows a detail of the low-energy region. A known contaminant is indicated by the filled circle.

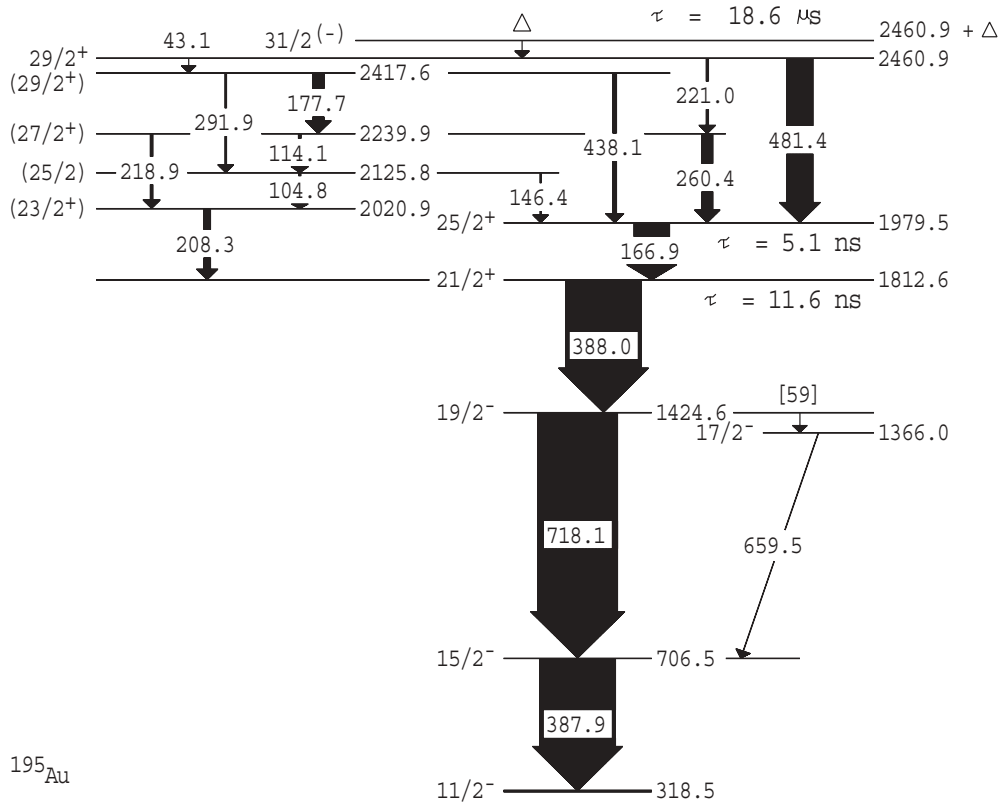

FIG. 2. Partial ^{195}Au level scheme, showing decays from the 19 μs isomer and branches from the states that it feeds, including members of the $h_{11/2}$ band. The widths of transitions are proportional to the delayed intensity. (See text for possible limits on the energy of the unobserved transition, Δ.)

the intensity observed in the present study proceeds through the decay of the $2461 + \Delta$ keV isomer. Part of our scheme is similar to that recently presented by Wang *et al*. [9], but there are several significant differences. Although the 2461-keV state, that decays mainly via the 481-keV transition, was assigned in both studies, a delayed component was not observed in Ref. [9] (presumably because their beam was not pulsed), and two additional branches from that state were assigned in the present work (221.0 and 43.1 keV). The other main differences with Ref. [9] appear to be the 292- and 438-keV γ rays identified here as branches from the 2418-keV state. The 438-keV branch to the $25/2^+$ state is important because it negates the $31/2^+$ assignment to the 2418-keV level suggested in Ref. [9], since the transition would then have to be an inordinately strong $M3$.

Reference [9] also assigned an $E3$ branch from the 1813-keV state to the 707-keV, $15/2^-$ level. We observe a corresponding 1106.2-keV line; however, its intensity is at the level of a possible sum γ ray. In terms of a strength, that would correspond to a moderately retarded $E3$ transition of $\leqslant$0.3 W.u.. A strong $E3$ decay is not expected given the configuration change. (Wheldon *et al*. [11] give a similar result.) Wang *et al*. [9] also place several transitions that would bypass the isomer observed here. In particular, they assign a 282-, 820-keV cascade feeding the 1426-keV, $19/2^-$ state. We have not been able to confirm this observation in our in-beam coincidence data.

The relative (delayed) intensities of transitions assigned to ^{195}Au are given in Table I.

A. Isomeric states

1. The 1813- and 1980-keV levels

A search was made for short lifetimes by projecting intermediate time differences with γ-ray gates on transitions above and below the state of interest. This technique is sensitive down to a region of about 1 ns for strong lines. The 1813-keV state has a reported *half*-life of 8(2) ns, corresponding to a mean-life of 12(4) ns.

Representative time spectra obtained using the time-γ-γ technique are given in Fig. 3. Figure 3(a) has (nominal) start and stop gates at 388 and 788 keV as indicated. Given the presence of two γ rays at 388 keV, this spectrum will contain effects due to the lifetimes of either the 707- or 1425-keV states (which will appear either left or right of zero, respectively). Since both states decay by relatively high-energy enhanced $E2$ transitions, their lifetimes will be short (subnanosecond). Hence, a fit to this spectrum can be used as one example of the energy-dependent prompt-timing response. The lifetime of the 1980-keV state can be extracted from the time spectrum of Fig. 3(b), constructed with gates on the 481-keV line directly feeding the state and the 167-keV deexciting γ ray. The fit to this spectrum includes a convolution with a prompt response

TABLE I. Properties of delayed transitions assigned to ^{195}Au.

E_γ[a]	I_γ	E_i	E_f	J_i^π	J_f^π
43.1	*4300(160)*[b]	2460.9	2417.6	$29/2^+$	$(29/2^+)$
59.0	*186(29)*[c]	1424.6	1366.0	$19/2^-$	$17/2^-$
104.8	339(34)	2125.8	2020.9	$(25/2^+)$	$(23/2^+)$
114.1	384(32)	2239.9	2125.8	$(27/2^+)$	$(25/2^+)$
146.4	184(25)	2125.8	1979.5	$(25/2^+)$	$25/2^+$
166.9	4475(128)	1979.5	1812.6	$25/2^+$	$21/2^+$
177.7	1464(59)	2417.6	2239.9	$(29/2^+)$	$(27/2^+)$
208.3	893(59)	2020.9	1812.6	$(23/2^+)$	$21/2^+$
218.9	377(35)	2239.9	2020.9	$(27/2^+)$	$(23/2^+)$
221.0	311(32)	2460.9	2239.9	$29/2^+$	$(27/2^+)$
260.4	1426(117)	2239.9	1979.5	$(27/2^+)$	$25/2^+$
291.9	216(29)	2417.6	2125.8	$(29/2^+)$	$(25/2^+)$
387.9	9323(181)[d]	706.5	318.5	$15/2^-$	$11/2^-$
388.0	9623(180)[d]	1812.6	1424.6	$21/2^+$	$19/2^-$
438.1	519(36)	2417.6	1979.5	$(29/2^+)$	$25/2^+$
481.4	3349(94)	2460.9	1979.5	$29/2^+$	$25/2^+$
659.5	186(29)	1366.0	706.5	$17/2^-$	$15/2^-$
718.1	10000(202)	1424.6	706.5	$19/2^-$	$15/2^-$

[a]Energies for strong transitions are accurate to about 0.1 keV.
[b]Total transition intensity; this value assumes $M1$ character for the subsequent 178-keV transition.
[c]Total transition intensity.
[d]Relative γ-ray intensity for unresolved doublet distributed allowing for difference in total conversion.

function. It suggests a mean-life of $\sim$5 ns for the state, although, at energies below about 200 keV, time walk and time distortion become more problematic, leading to a lower precision than is normally achievable. However, the spectrum of Fig. 3(c), produced by gating on the 481-keV γ ray and the 388-keV line, will contain the lifetimes of *both* the 1980- and 1813-keV states. In fact, this spectrum cannot be adequately fitted without inclusion of two lifetimes in sequence. Analysis of it and other spectra results in values of $\tau_m = 5.1(11)$ ns for the 1980 keV state and 11.6(4) ns for the 1813-keV state, as listed in Table II.

Note that mean-life obtained for the 1813-keV state from the present analysis agrees with that from previous work, even though the earlier studies were not cognisant of the short lifetime of the 1980-keV state. This does not constitute an inconsistency, since the earlier work would have been dominated by side-feeding at the 1813-keV level and, thus, would have been less sensitive to the short isomer that feeds it, in contrast to the present work where the feeding is essentially all from above.

TABLE II. Transition strengths and hindrances in ^{195}Au. (Alternative strengths for the decay of the 18.6 μs isomer are discussed in the text.)

E_γ (keV)	I_γ rel.	Final state	$\sigma\lambda$	α_T[a]	Strength (W.u.)
$E = 1980$ keV; $\tau = 5.1(11)$ ns; $J^\pi = 25/2^+$					
166.9	100(1)	$21/2^+$	$E2$	0.707	10.8(23)
$E = 1813$ keV; $\tau = 11.6(4)$ ns; $J^\pi = 21/2^+$					
388.0	100(1)	$19/2^-$	$E1$	0.0149	$4.21(16)\times10^{-7}$

[a]BRICC, Ref. [17].

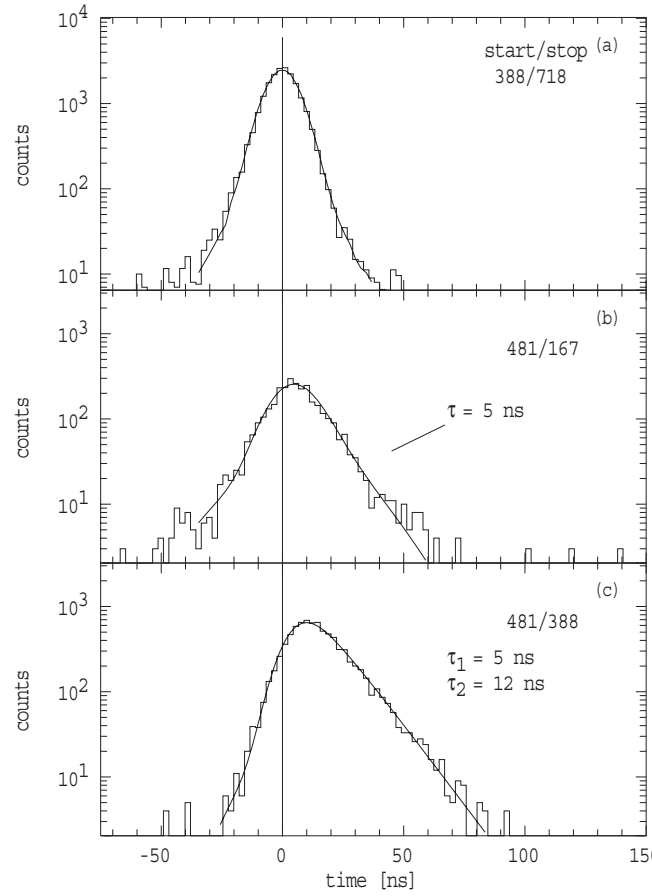

FIG. 3. Time spectra obtained with γ-ray gates as indicated, with fits including a prompt response function. Panel (a) is a representative "prompt" spectrum, panel(b) gives evidence for the lifetime of the 1980-keV state, and panel (c) is the corresponding spectrum for the 1813-keV level, fitted with a sequence of two isomers.

As can be seen from Table II, the 166.9-keV transition corresponds to an enhanced $E2$ decay with a strength of about 11 W.u. (to be discussed below), while the lifetime of the 1813-keV level arises from the hindered character of the 388-keV $E1$ transition. Its strength, of 4×10^{-7} W.u., is typical of $E1$ transitions in this region.

2. Isomer feeding the 2461-keV state

Analysis of the beam-correlated coincidence data suggests that, while the 2461-keV state is predominantly observed in the out-of-beam time region, there also is significant prompt component, amounting to about 15% of its population. Hence, the delayed component must be due to feeding from a higher-lying state. The mean-life of this upper isomer was deduced from a fit to the coincidence γ-ray intensities (gated on specific lines) in the macroscopically chopped data (see Fig. 4).

The feeding transition (indicated as Δ-keV) has not been identified, implying a low energy and/or high conversion. The

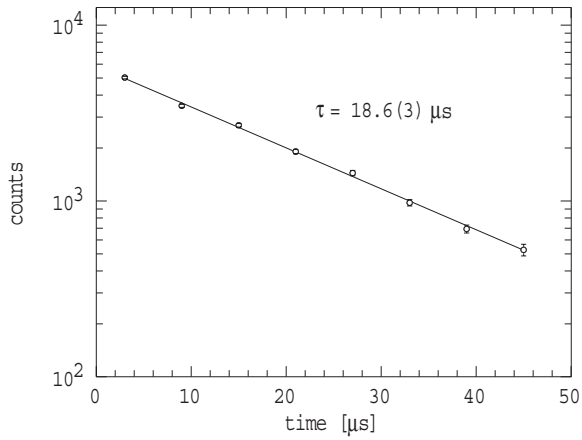

FIG. 4. Intensities as a function of time from γ-γ coincidence spectra selecting the main path in ^{195}Au, together with a fit returning the mean-life indicated.

sensitivity of the present experiment is at a level where strong $E1$ transitions down to ∼30–40 keV should be observed, but comparable $M1$ and $E2$ transitions become problematic below about 50 keV. Such unobserved low-energy transitions (often of $E2$ multipolarity), are common in this region. In particular, the fact that the 12^+ to 10^+ energy gap in the even-even neighbors is small, and the connecting transition was not observed, led in a number of cases to the misassignment of nanosecond lifetimes to 10^+ states, expected from the $h^2_{11/2}$ proton-hole configuration aligned to its maximum spin. Subsequently, several of these were attributed to 12^+ levels lying just above in excitation energy, produced from the alignment of a pair of $i_{13/2}$ neutron holes, giving rise to a multiplet with a close-lying pair of 10^+ and 12^+ states. Levon *et al*. [16] have recently evaluated lifetimes and g factors of the 10^+ and 12^+ states in even-even isotopes of Pt and Hg, addressing this issue. They also indirectly deduce an energy of 12.7(12) keV for the (proposed) unobserved transition in ^{194}Pt from an evaluation of the expected $12^+ \rightarrow 10^+$, $E2$ strength.

Superficially one might anticipate that the coupling of an $11/2^-$ proton to 10^+ and 12^+ core states could give rise to an isomer decaying via an unobserved $E2$ transition, equivalent to the low-energy $12^+ \rightarrow 10^+$ transition in the even-even neighbors. This alternative can be evaluated in detail by assuming that the $E2$ γ-ray strength of the unobserved transition would be comparable to that of the $12^+ \rightarrow 10^+$ γ-ray transition in ^{196}Hg, which is about 20 W.u.. The lifetime of a corresponding decay in ^{195}Au will depend predominantly on the energy and internal conversion. These have opposite energy dependencies that tend to balance each other, the main sensitivity being the proximity to the K and L edges. For a transition of the same $E2$ strength, the expected lifetime changes little for energies between the L_1 and K edges, varying from 17 ns to about 13 ns in the range 15–80 keV. The lifetime would rise if the energy were below the L edge, but only up to an approximate maximum of 316 ns at a minimum energy of, say, 2 keV.

Compensation of the γ-decay probability by the probability of internal conversion is similar, in fact, for $E1$, $M1$, $E2$, and $M2$ multipolarities in the 20–60 keV energy range. The observed lifetime of 18.6 μs implies strengths for a transition in this range of $\sim 1.5 \times 10^{-7}$ W.u. for an $E1$, $\sim 1.5 \times 10^{-6}$ W.u. for an $M1$, $\sim 1.7 \times 10^{-2}$ W.u. for an $E2$, and ∼0.5 W.u. for an $M2$ transition. As discussed above, an $E2$ decay of such a low strength would not be expected between related configurations. Similarly a very retarded $M1$ decay is unlikely, as is an $M2$ of single-particle strength. This leaves only the $E1$ alternative whose retarded strength is essentially typical (cf. the 388-keV transition in Table II). Based on the assignments to the lower states outlined in the following subsection, this will, therefore, lead to the suggested spin and parity of $31/2^{(-)}$ for the isomeric state.

B. Angular correlations, conversion coefficients, and spin assignments

Total conversion coefficients were extracted by analyzing various delayed intensity balances with specific γ-ray coincidence gates. The simplest cases involve the main cascade, although this is still complicated by the presence of the doublet of 388 keV lines. Nevertheless, it was possible to place a limit of $\alpha_T < 0.08$ on the upper 388-keV line deexciting the 1813-keV state assuming, as given by other evidence, that the lower line is indeed of $E2$ multipolarity. This is sufficient to eliminate a possible $M1$ multipolarity, leaving either $E1$ or $E2$ alternatives, the latter of which is not supported by the angular correlation information which indicates that one of the 388-keV transitions must be a stretched dipole [Fig. 5(a)]. This strongly supports the earlier proposal of $J^\pi = 21/2^+$ for the 1813-keV state.

The 166.9-keV feeding transition from the 1980-keV state has $\alpha_T = 0.72(6)$, which implies pure $E2$ character, given theoretical values of 0.11 for $E1$, 1.69 for $M1$, and 0.70 for $E2$ multipolarity. Together with the stretched quadrupole character favored by the angular correlation [Fig. 5(c)], this

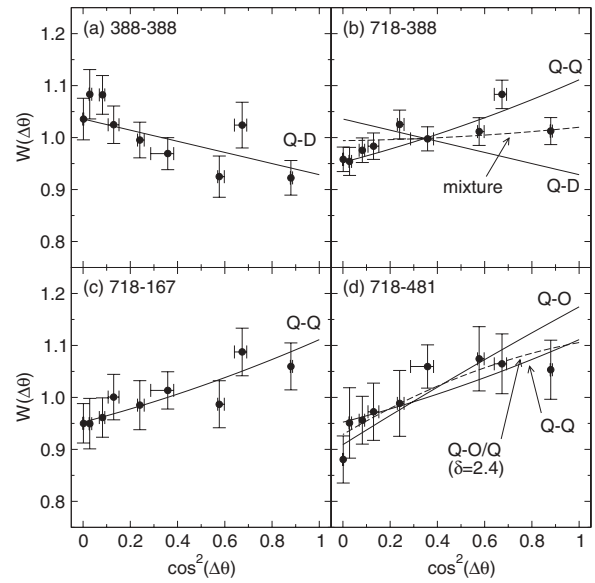

FIG. 5. Angular correlations with gates as indicated.

results in a firm spin and parity assignment of $25/2^+$ for the 1980-keV level.

Deduction of other conversion coefficients is complicated by the fragmented decay paths and the presence of a number of relatively low-energy lines leading to ambiguities in the balances, depending on the assumed multipolarities. From various evaluations, the 208.3-keV decay from the 2021-keV state to the $21/2^+$, 1813-keV level is limited to $\alpha_T = 0.06(10)$ and is, therefore, unlikely to be of pure $M1$ character, but could be either an $E1$, or more likely, a mixed $E2/M1$ transition. This is the basis of the tentative $(23/2^+)$ assignment to the 2021-keV state.

Above this, the 218.9-keV crossover transition in parallel with the 114.1- and 104.8-keV transitions is likely to be a stretched quadrupole. It could not be of $M2$ character since the 2240-keV level does not have a measurable lifetime, hence the proposed $(27/2^+)$ assignment for this state. The suggested spin and parity for the intervening 2126-keV state is $25/2$ but there is a residual ambiguity with the parity because the extraction of the conversion coefficients for the 104.8- and 114.1-keV transitions gave inconsistent values, depending on the approach used. The 260.4-keV branch from the 2240-keV level to the $25/2^+$ state at 1980 keV has an angular correlation suggesting a mixed dipole/quadrupole character, consistent with an $E2/M1$ multipolarity.

The 2126-keV state decays via a 291.9-keV transition; as is the case with the 218.9-keV γ ray, it could not be of $M2$ multipolarity, but is probably of stretched $E2$ character. The main branch at 177.7 keV has $\alpha_T = 1.8(3)$, which is close to the $M1$ value, consistent with a $(29/2^+)$ assignment for the 2418-keV state. This is further supported by the observation of the 438.1-keV branch to the $25/2^+$, 1980-keV state. It is not possible to get a precise value for the lifetime of the 2418-keV level since it is essentially completely fed by the long isomer, and the connecting transition is of very low energy. Nevertheless, the fact that the 43.1-keV transition is observed in "prompt" coincidence implies a lifetime of $\lesssim$100 ns for the 2418-keV intermediate state.

The state at 2461 keV has three decay branches assigned, at 43.1, 221.0, and 481.4 keV. Because of the low energy of the 43.1-keV transition, its conversion coefficient is difficult to extract: The approximate value obtained falls between the $E1$ prediction (0.8) and the expected $M1$ value (15.2). The efficiency at such a low energy is uncertain, but it is more likely to be overestimated, since most conceivable effects (absorption, time walk, time restrictions, etc.) that might not be fully accounted for in the efficiency evaluation are more likely to reduce the apparent intensity. A correction in this direction would slightly favor $E1$ character, rather than the assigned $M1$ multipolarity. However, we have not been able to fully quantify this possibility. The conversion for the 221.0-keV transition is also uncertain since there are parallel branches in to the 2240-keV state that it populates.

The 481.4-keV line is of too high an energy to obtain its conversion. While its angular correlation is not precisely determined, it does favor either a stretched quadrupole or alternatively a mixed octupole/quadrupole character, although a stretched octupole possibility cannot be excluded, as indicated in Fig. 5(d). In the absence of a significant lifetime for the 2461-keV state, $M2$ and $E3$ multipolarities can be eliminated, leaving $E2$ as the acceptable alternative and a proposed assignment of $J^\pi = 29/2^+$ for the 2461-keV level. In this case, a branch to the 2126-keV state might have been expected if that state had positive parity, but such a branch was not observed.

Although it is not supported by the observation of prompt feeding, if the lifetime had been attributable to the 2461-keV state, rather than feeding from a higher state, the correlation analysis and transition strengths would also have favored a $31/2^-$ assignment for the isomer, in that case with $E3$ character for the 481.4-keV transition, and a strength of 2.5 W.u.. The strengths implied for the other branches would have been $\sim 4 \times 10^{-8}$ W.u. for a 43.1-keV $E1$ branch and $\sim 5 \times 10^{-3}$ W.u. for a 221-keV $M2$ branch.

IV. POTENTIAL ENERGY SURFACE CALCULATIONS

Calculations allowing for self-consistent shape changes for a range of odd-A iridium isotopes were reported in our Ref. [6]. These have been extended to the gold isotopes. The most likely three-quasiparticle configurations were computed using the method of K-constrained diabatic potential-energy surfaces [18,19] with a nonaxial deformed Woods-Saxon potential and approximate particle-number projection achieved through the Lipkin-Nogami prescription. The results for selected states (mainly the highest-spin, lowest-energy levels predicted) are listed in Table III.

In progressing from the iridium isotopes to the equivalent gold cases, it becomes clear from the present evaluations that the tracking of particular configurations and the associated minima becomes more challenging. A number of the configurations with clear minima in the iridium cases do not give minima in ^{195}Au. Several examples of these are marked in Table III. For the same reasons, there is an implicit (imprecise) uncertainty in the predicted energies when the mimina become very shallow.

Note also that the TRS calculation of the lowest negative-parity sequences in a range of gold isotopes indicates well defined mimima at about $\gamma = -70^\circ$; this is slightly triaxial, but beyond the purely oblate axis (see Fig. 3 of Ref. [9]).

V. DISCUSSION

A. Systematics

The systematics of selected states in the $N = 116$ isotones of relevance is summarized in Fig. 6, including the present results. In this figure, the schemes have been shifted so that the ground states in the even-even neighbors align with the $11/2^-[505]$ bandhead in the odd-proton cases. Short-lived 12^+ isomers are now known in all the even-even cases (see Refs. [20,21] for recent results on ^{192}Os), while the negative-parity sequences (5^-, 7^-, 9^-, . . . , etc.) are well studied.

As indicated earlier, one focus in the odd-proton cases has been the relationship between the three-quasiparticle states, such as a $31/2^+$ isomer, and the two-particle (proton and neutron) structures systematically observed in the even-even Pt and Hg cores (see, for example, Refs. [9,10,22–25]). The results of g-factor measurements led to the conclusion that

TABLE III. Selected three-quasiparticle configurations in ^{195}Au with calculated equilibrium energies and deformations.

K^π	Configuration	β_2	γ (deg.)	β_4	$E^{\text{cal.}}$(keV)
$17/2^-$	$\nu 11/2^+[615],3/2^-[512]\otimes\pi 3/2^+[402]$	0.121	29	−0.033	1238
$21/2^-$	$\nu 11/2^+[615],7/2^-[503]\otimes\pi 3/2^+[402]$				[a]
$21/2^-$	$\nu 11/2^+[615],9/2^-[505]\otimes\pi 1/2^+[400]$	0.081	2.5	−0.000	1976
$23/2^+$	$\nu 11/2^+[615],1/2^-[510]\otimes\pi 11/2^-[505]$	0.142	29	−0.037	2863
$23/2^-$	$\nu 11/2^+[615],9/2^-[505]\otimes\pi 3/2^+[402]$	0.115	40	−0.026	1653
$25/2^+$	$\nu 11/2^+[615],3/2^-[512]\otimes\pi 11/2^-[505]$	0.148	30.6	−0.038	2156
$27/2^+$	$\nu 11/2^+[615],13/2^+[606]\otimes\pi 3/2^+[402]$	0.148	33.8	−0.078	2872
$29/2^+$	$\nu 11/2^+[615],7/2^-[503]\otimes\pi 11/2^-[505]$				[a]
$29/2^-$	$\nu 9/2^+[624],11/2^+[615]\otimes\pi 9/2^-[514]$	0.094	25	−0.017	2668
$31/2^-$	$\nu 9/2^+[624],11/2^+[615]\otimes\pi 11/2^-[505]$	0.141	30.4	−0.029	2979
$31/2^+$	$\nu 11/2^+[615],9/2^-[505]\otimes\pi 11/2^-[505]$				[a]
$33/2^-$	$\nu 11/2^+[615],13/2^+[606]\otimes\pi 9/2^-[514]$				[a]
$35/2^-$	$\nu 11/2^+[615],13/2^+[606]\otimes\pi 11/2^-[505]$				[a]

[a]No minimum found.

the isomers observed are generally formed by two-neutron, one-proton configurations [24] and, specifically, that the g factor for the $31/2^+$ isomer in ^{191}Au is consistent with that expected for an $h_{11/2}$ proton coupled to a 10^- neutron core. At lower spin, the $21/2^+$ isomer in ^{195}Au was suggested to arise from a coupling of the $11/2^-$ proton to the 5^- two-neutron-hole state known in the even-even neighbors. That assignment for the $21/2^+$ state is supported by the present evaluations, which confirm its spin and parity and show that the $E2$ decay strength is consistent with that in the core.

At first sight, the systematic trends might encourage association of the observed isomer in ^{195}Au with the 180 μs isomer in ^{193}Ir, but, aside from the obvious inconsistency with the spin and parity, this is not predicted from detailed calculations on the expected three-quasiparticle states, at least partly because of configuration-dependent shape differences.

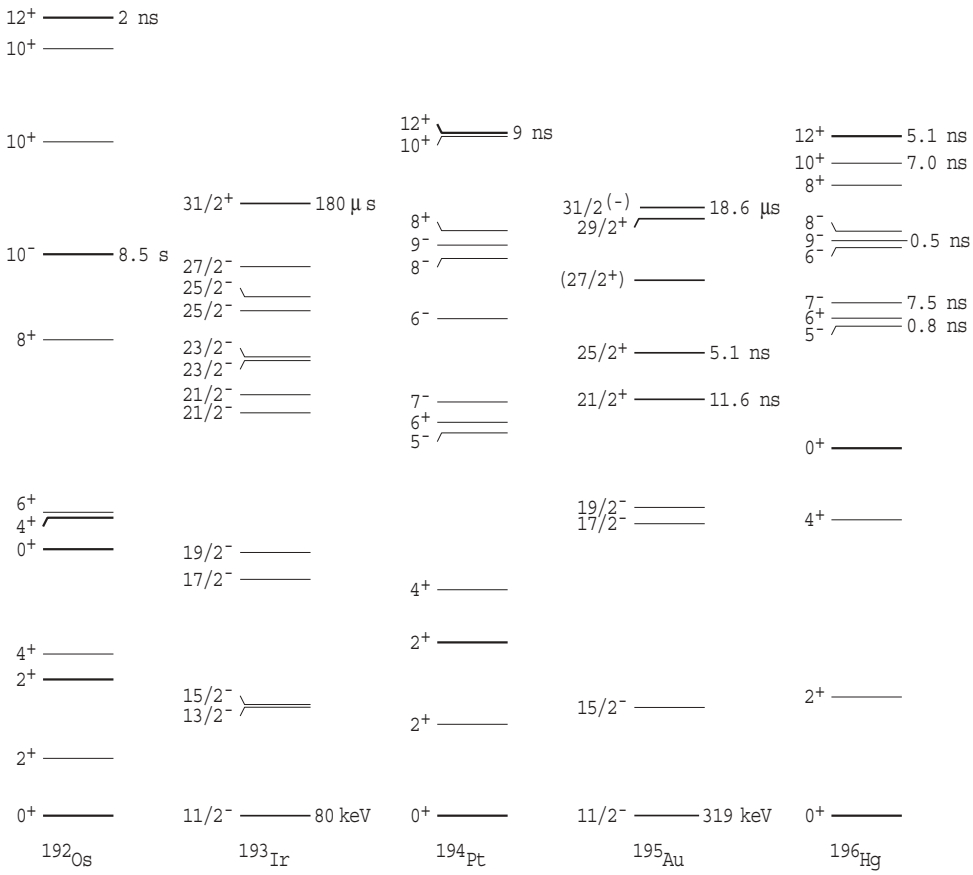

FIG. 6. Energy systematics of selected intrinsic and collective states in the $N = 116$ isotones. The energies of states in the odd-proton cases ^{193}Ir and ^{191}Ir have been lowered so that the $11/2^-[505]$ bandheads coincide with the ground states of the even-even cases.

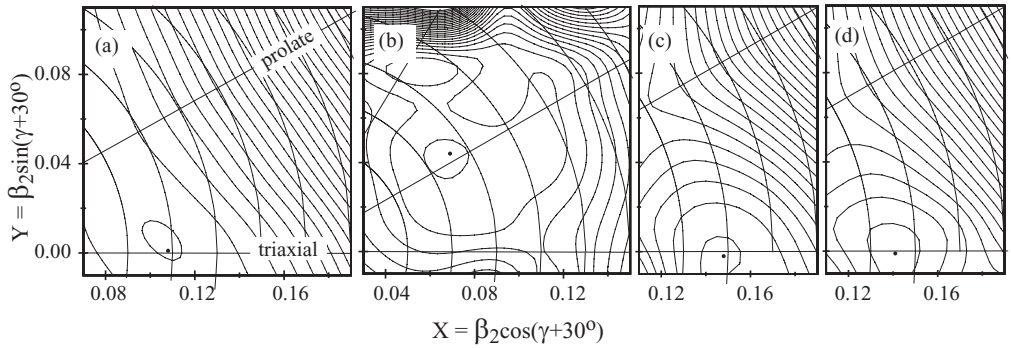

FIG. 7. Potential energy surfaces for selected configurations in ^{195}Au. These correspond to (a) the $3/2^+$ ground state and three-quasiparticle states listed in Table III with (b) $J^\pi = 21/2^-$, (c) $J^\pi = 25/2^+$, and (d) $J^\pi = 31/2^-$, as discussed in the text. The contour separation is 200 keV.

B. Configurations and equilibrium shapes

As can be seen from Table III, nearly all intrinsic configurations likely to produce relatively low-lying states are predicted to be triaxial ($\gamma \sim 30^\circ$), a significant exception being the $21/2^-$ state expected at 1976 keV which essentially corresponds to the $1/2^+[400]$ proton coupled to the 10^- neutron core configuration. It tends to favor a prolate deformation (γ is small, $\sim 3^\circ$), but as can be seen from the PES in Fig. 7(b), the potential energy surface is very shallow and poorly defined. In contrast, the one-quasiparticle ground state has a minimum at a triaxial shape, but again with a very shallow valley in the gamma direction.

Several of the important high-spin configurations, in particular the $31/2^+\nu 11/2^+[615]$, $9/2^-[505] \otimes \pi 11/2^-[505]$ combination corresponding to the coupling of the $11/2^-[505]$ proton to the 10^- neutron core state, do not produce detectable minima in the present calculations. In contrast, this configuration does minimize at triaxial deformation in the equivalent calculations for the isotone ^{193}Ir, and we have, in fact, associated it with the long-lived isomer in ^{193}Ir [6]. The other case of interest in this context is the $35/2^-$ state obtained by coupling the $11/2^-[505]$ proton to the 12^+ neutron core. Again, no minimum is obtained in ^{195}Au, unlike the prediction of a well defined low-lying state in ^{193}Ir. (The possibility of a low-lying $35/2^-$ state will be discussed further below.)

We propose to associate the $31/2^-$, three-quasiparticle state of Table III, calculated to lie at 2979 keV, with the $31/2^-$ isomer observed experimentally at $2461 + \Delta$ keV. This configuration corresponds to coupling of an $11/2^-[505]$ proton to the two-neutron 10^+ core, and according to the calculations is moderately deformed ($\beta_2 = 0.142$) and essentially triaxial, with $\gamma = 30^\circ$. In the iridium isotone, this configuration was also calculated to be competitive in energy with the observed $31/2^+$ isomers, but it was not identified [6]. The main issue with this assignment is that the predicted energy is higher than the observed state by about 500 keV, while agreement in other cases has usually been within roughly 200 keV. The $25/2^+$ state calculated at 2156 keV, for example, can be associated with the 1980-keV experimental state.

Considering the other calculated three-quasiparticle intrinsic states that might be observed, and remembering that all will have to compete with collective states such as the members of the $11/2^-[505]$ band, the only one of interest is possibly the weakly deformed $23/2^-$ level predicted at the relatively low energy of 1653 keV. Its configuration is related to the predicted $31/2^+$ state, being essentially the $3/2^+[402]$ proton coupled to the same 10^- two-neutron core that gives rise to the long-lived 10^- isomer in ^{192}Os. Note, however, that an equivalent 10^- state is not known in the less-deformed, even-even neighbor ^{194}Pt.

As mentioned in the introduction, several spherical configurations could, in principle, give rise to positive-parity states, particularly $29/2^+$ and $33/2^+$ states that might be in the region of interest. While these cannot be treated fully in the present model, their energies can be estimated by fixing the shape at sphericity. This approach gives predicted energies of 1938 keV for the $29/2^+$ state and 3653 keV for the $33/2^+$ level. The latter would not be of interest, but the $29/2^+$ state could be a candidate for the observed $(29/2^+)$ state at 2418 keV.

Empirically, this is, in fact, just the combination of the 9^-, two-neutron core state and the $11/2^-[505]$ proton. As can be seen from Fig. 6, the energy of the 9^- state (adjusted for the excitation energy of the proton) is close to that of the 2418-keV state in both ^{194}Pt and ^{196}Hg. The averaged energy (with 319 keV added) is 2375 keV, strong support for this association. Note that in Ref. [9] the 2418-keV state was suggested to be the anticipated $31/2^+$ state, while the 2240-keV level, assigned here as $27/2^+$, was proposed as the $29/2^+$ member of a band based on the 1813-keV, $21/2^+$ state. The present view, however, is that the 1813-, 1980-, and 2418-keV states, assigned as $21/2^+$, $25/2^+$, and $29/2^+$ in our study, should be associated with the 5^-, 7^-, and 9^- states of the core. This is in good agreement with the averages of the ^{194}Pt and ^{196}Hg excitation energies, adjusted by adding 319 keV for the proton excitation, which gives energies of 1885, 1982, and 2375 keV for these three levels.

The other levels to be expected in this picture are $23/2^+$ and $27/2^+$ states obtained by weak coupling to the 6^- and 8^- core states. These could provide an explanation for the 2021- and 2240-keV experimental states [$(23/2^+)$ and

$(27/2^+)$, respectively] although their energies are in somewhat poorer agreement with the averaged core levels which would correspond to 2240 and 2368 keV. This might be less of an issue than at first sight since the configurations of the even-spin states might be less pure.

Several qualifications are necessary here. As discussed in detail by Levon *et al*. [16] in the context of measured g factors and the associated wave functions, significant changes occur in the configurations of the even-even nuclei. Principally these are (i) that the 7^- states change in character from a largely proton structure in platinum to predominantly neutron structure in mercury; (ii) the 10^+ state in ^{194}Pt is from the $\pi h_{11/2}^{-2}$ multiplet, but the 12^+ isomer is from the $\nu i_{13/2}^{-2}$ multiplet whereas, in ^{196}Hg, both are from the neutron configuration; and (iii) the observed (relatively low-lying) 8^+ state in ^{194}Pt is a collective state associated with the ground state, whereas it is a member of the 8^+, 10^+, 12^+ multiplet in ^{196}Hg, although the purity of its wave function is unknown.

These issues are important for understanding the low energy and isomeric nature of the $31/2^-$ state under discussion. The logical conclusion from the arguments given earlier regarding the positive-parity states is that the $31/2^-$ state has, in essence, the configuration of the $11/2^-[505]$ proton coupled to the 10^+ core state, although the expected energy of these, estimated using the earlier approach, would be at about 2700 keV. Part of the significantly lower energy could be attributed to the deformation; however, an important factor will be the residual proton-neutron interaction which is not contained, at least not explicitly, in the PES calculations.

C. Semi-empirical shell model

In a spherical situation, the interaction between mutually aligned high-spin neutrons and protons is large, providing they are of the same character (predominantly holes in this case) and this would significantly depress both the $31/2^-$ and $35/2^-$ states obtained by coupling the $h_{11/2}$ proton hole to the 10^+ and 12^+ $i_{13/2}^{-2}$ multiplet states. As discussed in detail in Sec. III A2, if the $35/2^-$ state lies above the $31/2^-$ level, it would not lead to a long isomer since it could then decay by a low-energy, but enhanced, $E2$ transition to the $31/2^-$ level, and would not be visible because of the long lifetime of the lower state. Furthermore, this $31/2^-$ state could only be long-lived (as observed) if the $27/2^-$ multiplet member did not fall below it in energy.

The situation is complementary to that analyzed for the $J^\pi = 31/2^-$ isomer in ^{189}Pb (Ref. [26]). In that case, an $i_{13/2}$ neutron is coupled to an aligned two-proton configuration. The corresponding residual interaction controls the ordering of the lowest high-spin states in the multiplet, as a function of the Fermi level position within the $i_{13/2}$ neutron shell, resulting in more attractive interactions when the neutron is particle-like. In the present case, since the $h_{11/2}$ proton can be assumed to be largely hole-like, the strongest attractive interactions occur when the $i_{13/2}$ neutron is also hole-like. Figure 8 shows the result of a calculation based on the formalism described in Ref. [26], appropriately adjusted for the difference in proton character, and using the residual interactions for coupling of the $h_{11/2}$ proton hole to the $i_{13/2}$ neutron [27,28] adopted

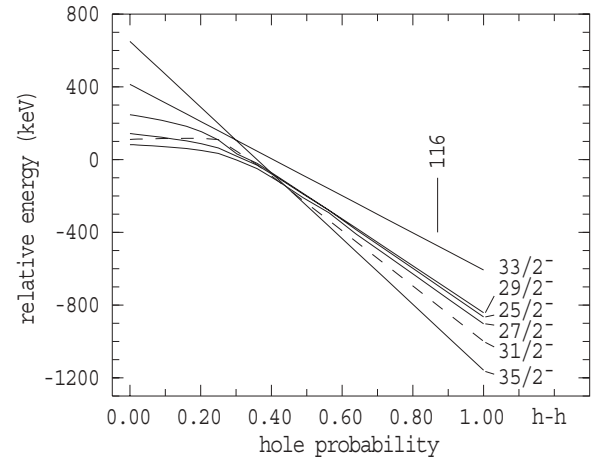

FIG. 8. Dependence of the relative energies of high-spin states due to the residual interaction within the $\nu i_{13/2}^2 \times \pi h_{11/2}^{-1}$ multiplet as a function of the hole nature of the $i_{13/2}$ neutrons (assuming a pure hole character for the $h_{11/2}$ proton). The hole probability for $N \sim 116$ is indicated.

in the study of nuclei near ^{208}Pb [27]. A few of the matrix elements (those for spins 12^-, 11^- and 10^-) are derived from experiment (see Ref. [29]) and others were obtained from a recent adjustment of theoretical values [27,28].

The key points to take away from Fig. 8 are that, once the $i_{13/2}$ neutron becomes more hole- than particle-like (probability squared of $U^2 > 0.5$), the $31/2^-$ state (dashed line) is predicted to always lie below the lower-spin members, hence decays to them would not be possible. The $35/2^-$ state is the most favored and is predicted to fall significantly below the $31/2^-$ level at 60% hole character. This would have two consequences: first, it would provide an alternative decay path for the $31/2^-$ state, hence that state would not be a long-lived isomer; and, second, the $35/2^-$ state itself would have no feasible γ-ray decay paths, leading presumably to a very long-lived isomer that would prefer to β decay. (The situation of possible very low-lying β-decaying isomeric states was also discussed for the iridium cases [6].)

However, since this approach assumes shell-model configurations, it is likely to lead to an overestimate of the magnitude of the residual interactions given that nuclear shape distortions (and vibrations) must play a role; i.e., the configurations will not be pure. Nevertheless, even if the interactions are diluted in magnitude, there will still remain attractive interactions that could explain the observed states. Note also that the nominal position of the Fermi level would lead to $i_{13/2}$ neutrons that are $\sim$80% hole-like, as indicated in Fig. 8, although, again, this depends in detail on the level orderings and local level densities which are also affected by the nuclear shape. The positive-parity states obtained by coupling an $h_{11/2}$ proton to the $f_{7/2}$ and $h_{9/2}$ neutron holes (giving rise to the 9^- states in the core nuclei, for example) can also be treated in a similar fashion and, in those cases, the predicted interactions are smaller in magnitude, but still significant.

More extensive calculations beyond the scope of the present study would be required to examine such spherical and deformed states in detail, within a consistent framework.

VI. SUMMARY AND CONCLUSIONS

Excited states in the transitional nuclide ^{195}Au have been populated and studied using multinucleon transfer reactions with an energetic ^{136}Xe beam and γ-ray spectroscopy. The new results include characterization of the known $25/2^+$ state at 1780 keV and identification of an isomer with $\tau = 18.6(3)\,\mu$s at $2461 + \Delta$ keV, with a complex decay path through newly identified excited states. Three of these can be related to the 5^-, 7^-, and 9^- states known in the even-even core nuclei. Spins and parities have been constrained through consideration of total conversion coefficients, angular correlations, and transition strengths. The uppermost isomer has been assigned a likely spin and parity of $J^\pi = 31/2^-$ although there remain some ambiguities in this assignment.

Configuration-constrained calculations suggest that deformations in this transitional nucleus depend sensitively on the populated orbitals, apparently more so than in the lower-Z isotone ^{193}Ir. Not all configurations produce significant minima in the model calculations for ^{195}Au. From a shell-model point of view, the key factors governing the disposition of high-spin multiparticle states that could control the formation of isomers are the residual interactions that depend on the particle and hole character of the constituents.

This sensitivity and apparent difference between the isotones serves to underline the point that extrapolations on the basis of systematics are likely to be unreliable in nuclei where the shape depends strongly on the configuration. This will be a continuing issue in tracing multi-quasiparticle nuclear structure properties in this region.

ACKNOWLEDGMENTS

G.D.D. is grateful to K. H. Maier for providing matrix elements used in this study. This work was supported by the Australian Research Council Grants No. DP0986725, No. DP03445844, and No. FT100100991, and by the US Department of Energy, Office of Nuclear Physics, under Contract No. DE-AC02-06CH11357 and Grant No. DE-FG02-94ER40848.

[1] D. Cline, Annu. Rev. Nucl. Part. Sci. **36**, 683 (1986).
[2] L. M. Robledo, R. Rodriguez-Guzman, and P. Sarriguren, J. Phys. G **36**, 115104 (2009).
[3] P. Sarriguren, R. Rodriguez-Guzman, and L. M. Robledo, Phys. Rev. C **77**, 064322 (2008).
[4] P. Möller, J. R. Nix, W. D. Myers, and W. J. Swiatecki, At. Data Nucl. Data Tables **59**, 185 (1995).
[5] P. Möller, R. Bengtsson, B. G. Carlsson, P. Olivius, T. Ichikawa, H. Sagawa, and A. Iwamoto, At. Data Nucl. Data Tables **94**, 758 (2008).
[6] G. D. Dracoulis *et al.*, Phys. Lett. B **709**, 59 (2012).
[7] P. O. Tjøm, M. R. Maier, D. Benson Jr., F. S. Stephens, and R. M. Diamond, Nucl. Phys. A **231**, 397 (1974).
[8] F. S. Stephens, Rev. Mod. Phys. **47**, 43 (1975).
[9] S. C. Wang *et al.*, Phys. Rev. C **85**, 027301 (2012).
[10] Y. Gono, R. M. Lieder, M. Müller-Veggian, A. Neskakis, and C. Mayer-Böricke, Nucl. Phys. A **327**, 269 (1979).
[11] C. Wheldon *et al.*, Phys. Rev. C **74**, 027303 (2006).
[12] R. Broda, J. Phys. G **32**, R151 (2006).
[13] G. D. Dracoulis *et al.*, Phys. Rev. C **71**, 044326 (2005)
[14] G. J. Lane *et al.*, Phys. Rev. C **82**, 051304(R) (2010).
[15] R. V. F. Janssens and F. S. Stephens, Nucl. Phys. News **6**, 9 (1996).
[16] A. I. Levon, Yu. V. Nosenko, V. A. Onischuk, A. A. Schevchuk, and A. E. Stuchbery, Nucl. Phys. A **764**, 24 (2006).
[17] T. Kibédi, T. W. Burrows, M. B. Trzhaskovskaya, P. M. Davidson, C. J. Nestor Jr., Nucl. Instrum. Methods A **589**, 202 (2008).
[18] F. R. Xu, P. M. Walker, J. A. Sheikh, and R. Wyss, Phys. Lett. B **435**, 257 (1998).
[19] F. R. Xu, Chin. Phys. Lett. **18**, 750 (2001).
[20] G. D. Dracoulis *et al.*, Proceedings of the Rutherford Centennial Conference on Nuclear Physics, 8–12 August 2011 [J. Phys. Conf. Ser. **381**, 012060 (2012)].
[21] G. D. Dracoulis *et al.* (unpublished).
[22] V. Kölschbach, P. Scholer, K. Hardt, D. Rosendaal, C. Günther, K. Euler, R. Tijlle, M. Marten-Tolle, and P. Zeyen, Nucl. Phys. A **439**, 189 (1985).
[23] Ts. Venkova *et al.*, Z. Phys. A **344**, 231 (1992).
[24] N. Perrin, C. Bourgeois, A. Korichi, M. Pautrat, H. Sergolle, N. Barré, C. Vieu, N. Benouaret, and J. Vanhorenbeeck, Z. Phys. A **359**, 373 (1997).
[25] Y. Oktem *et al.*, Phys. Rev. C **76**, 044315 (2007).
[26] G. D. Dracoulis, G. J. Lane, T. Kibédi, and P. N. Nieminen, Phys. Rev. C **79**, 031302(R) (2009).
[27] K. H. Maier and M. Rejmund, Eur. Phys. J. A **14**, 349 (2002).
[28] K. H. Maier (private communication).
[29] B. Szpak *et al.*, Phys. Rev. C **83**, 064315 (2011).